RSC Advances

PAPER

View Article Online
View Journal | View Issue



Cite this: *RSC Adv.*, 2016, **6**, 6205

# Self-powered, ultraviolet-visible perovskite photodetector based on $TiO_2$ nanorods

Hai Zhou,[a] Zehao Song,[a] Pan Tao,[a] Hongwei Lei,[b] Pengbin Gui,[a] Jun Mei,[a] Hao Wang*[a] and Guojia Fang[b]

Received 28th December 2015
Accepted 6th January 2016

DOI: 10.1039/c5ra27840f

www.rsc.org/advances

A self-powered, ultraviolet-visible perovskite photodetector based on $TiO_2$ nanorods/$CH_3NH_3PbI_3$ heterojunction was reported. We found that the device showed good photovoltaic properties with a short-circuit current density of 17.83 mA $cm^{-2}$, an open-circuit voltage of 0.76 V and a fill factor of 51.34%, leading to a PCE of 6.95%. Based on the wide band gap and the perovskite supporting part of the $TiO_2$ nanorods, the device showed good ultraviolet-visible photo-response characteristics with the responsivity at zero bias reaching ~0.26 and 0.85 A $W^{-1}$ at 364 and 494 nm, respectively. These results present potential applications of $TiO_2$/perovskite photodetectors in ultraviolet and visible regions.



## I. Introduction

Organic–inorganic hybrid materials, particularly the perovskite family, have shown great promise for use in field-effect transistors, light-emitting diodes, sensors, and photodetectors for more than a decade.[1] Recently, with the power conversion efficiency (PCE) of lead halide perovskite ($CH_3NH_3PbX_3$, X = Cl, Br, I)-based thin film photovoltaic devices reaching more than 19.3%,[2] organic–inorganic perovskites have attracted more and more attention as light-harvesting materials for mesoscopic solar cells with enhanced performance due to their suitable band gap, high absorption coefficient (>$10^4$ $cm^{-1}$), double carrier transport properties and good tolerance for impurities and defects.[3–7] For photodetectors, the organic–inorganic perovskites are also very good for the visible detection with the simple preparation process and low power consumption. Y. Yang reported the perovskite photodetector based on $CH_3NH_3PbI_{3-x}Cl_x$, the device showed exhibit a large detectivity approaching $10^{14}$ Jones, which is about one order of magnitude higher than the detectivity of a Si photodetector in the same spectral region.[8] The perovskite photodetector based on flexible ITO coated substrate was also reported and its photoresponsivity reaches to 3.49 and 0.0367 A $W^{-1}$ with an external quantum efficiency of 1.19 × $10^3$%, 5.84% at 365 nm and 780 nm with a voltage bias of 3 V, respectively.[9]

Nowadays, self-powered nanodevices and nanosystems have attracted increasing attentions due to its self-conficient characteristic, which can function well without an external power source.[10,11] For most of the traditional PDs, they need an external electric field to drive the photogenerated carriers to generate photocurrent. As a novel self-powered PD based on the photovoltaic effect, it can be operated at zero bias without consuming external power. So it is highly desirable to meet the demands of the energy shortage. In this work, $CH_3NH_3PbI_3/TiO_2$ nanorods self-powered PDs were fabricated by a facile and low-cost process and their ultraviolet (UV)-visible detection characteristics were investigated. Herein, the $TiO_2$ nanorods are prepared by hydrothermal synthesis method on FTO substrate directly without a seed layer, which simplifies the fabrication process of the device. And therein, the $TiO_2$ nanorods are important for two aspects: one is can be a ultraviolet (UV) response layer for their wide band gap semiconductor (~3.2 eV). The other is a supporting part for the perovskite.

## II. Experiment

### The synthesis of $TiO_2$ nanorods

The FTO substrates were initially cleaned with acetone, ethanol and deionized water, respectively, and then blown dry with dry $N_2$. Then $TiO_2$ nanorods were grown on FTO substrates without a $TiO_2$ seed layer by hydrothermal synthesis method. The details of the hydrothermal conditions for obtaining $TiO_2$ nanorods are below: in brief, 8 ml of deionized water was mixed with 8 ml of concentrated hydrochloric acid (36.5–38% by weight) and the mixture was stirred in the air for 5 min. After that, 0.3 ml of titanium butoxide was added and the solution was stirred for another 5 min, then it was placed in a Teflon-lined stainless steel autoclave. Then, the FTO substrate was placed in. The hydrothermal synthesis was conducted at 150 °C for 3 h in an electric oven.

[a]*Hubei Collaborative Innovation Center for Advanced Organic Chemical Materials, Hubei Key Laboratory of Ferroelectric and Dielectric Materials and Devices, Faculty of Physics and Electronic Science, Hubei University, Wuhan 430062, China. E-mail: nanoguy@126.com*

[b]*Key Lab of Acoustic and Photonic Materials and Devices of Ministry of Education, Department of Electronic Science & Technology, School of Physical Science & Technology, Wuhan University, Wuhan, 430072, P. R. China*

### Perovskite device fabrication

Organohalide lead perovskite ($CH_3NH_3PbI_3$) was synthesized using the method described by Lee *et al.* $CH_3NH_3I$ was synthesized firstly. Generally, hydroiodic acid (30 ml, 0.227 mol, 57 wt% in water, Aldrich) and methylamine (27.8 ml, 0.273 mol, 40% in methanol, TCI) were mixed and stirred in the ice bath for 2 h. After stirring at 0 °C for 2 h, the resulting solution was evaporated at 50 °C for 1 h and generated chemicals ($CH_3NH_3I$). The precipitate was washed three times with diethylether, dried under vacuum and used without further purification. 1 M $PbI_2$ (dissolved in *N*,*N*-dimethylformamide (DMF) at 70 °C for 12 h) was spin coated onto the $TiO_2$ nanorods at a speed of 2000 rpm for 60 s and was heated at 70 °C for 30 min. Subsequently, the film was dipped into a solution of $CH_3NH_3I$ (10 mg $ml^{-1}$, dissolved in isopropanol) for 2 min. Then, the film was thermally annealed at 70 °C in the air for 30 min. After the deposition of perovskite materials, a hole transport layer (HTL) solution, which consisting of 55 mM TBP, 26 mM Li-TFSI, and 68 mM spiro-OMeTAD dissolved in acetonitrile and chlorobenzene (1 : 10, v/v), was coated on the $TiO_2$ film by spin-coating at a speed of 2000 rpm for 30 s. Finally, the electrode was deposited by thermal evaporation of gold under a pressure of $5 \times 10^{-5}$ Torr. The active area was 0.09 $cm^2$.

The morphology was observed by Sirion field emission scanning electron microscopy (SEM) (Philips XL30). The PV characteristics were measured with a Keithley 236 source-measurement unit under 100 mW $cm^{-2}$ using an AM 1.5G standard Newport #96000 Solar Simulator. The photosensitivity was performed by using 66984 Xe arc source (300 W Oriel) and Oriel Cornerstone™ 260 1/4 m Monochromator. The sample was under illumination directly (parallel with the nanorods) and the optical power of light was measured by a UV-enhanced Si detector. All the *I*–*V* characteristics were measured by a Keithley 4200 electrometer.

## III. Results and discussion

In our experiment, the SEM images of $TiO_2$ nanorods are shown in Fig. 1(a) and (b), which are the top and cross-sectional views of the as-prepared $TiO_2$ nanorods on FTO substrate, respectively. From the photographs, a 400 nm $TiO_2$ film was seen between the $TiO_2$ nanorods and FTO substrate. Also, the $TiO_2$ nanorods grow vertically on the $TiO_2$ film and the gap between $TiO_2$ nanorods is very big, and the average diameter and length of these $TiO_2$ nanorods are around 200 nm and 2 μm. The existence of the $TiO_2$ film may be attributed to the hydrothermal synthesis method. Before the growth of the $TiO_2$ nanorods, the $TiO_2$ seed layer will be formed first under the hydrothermal conditions. Then with the increase of time, the $TiO_2$ nanorods begin to grow on the $TiO_2$ film. Herein, the $TiO_2$ film will prevent from perovskite contacting with the FTO, which will result in a big photo-current. The top view of $CH_3NH_3PbI_3$ film is shown in Fig. 1(c). From the photograph, we can see the $CH_3NH_3PbI_3$ film is very flat and uniform, also we can see the $CH_3NH_3PbI_3$ film is completely filled and the ZnO nanorods can not be seen. Fig. 1(d) shows the absorption of the $TiO_2$ nanorods and the $CH_3NH_3PbI_3$ on $TiO_2$ nanorods/FTO. The absorption spectrum of the $CH_3NH_3PbI_3$ on $TiO_2$ nanorods/FTO shows a strong absorption from the near-IR region to 400 nm, which mainly comes from $CH_3NH_3PbI_3$. And the absorption in UV region is mainly attributed to $TiO_2$ nanorods.

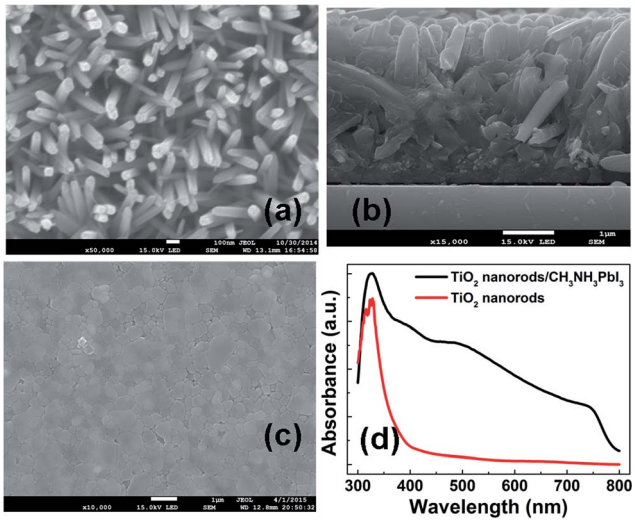


Fig. 1 The top (a) and cross-sectional (b) views of the SEM photograph of the as-prepared $TiO_2$ nanorods on FTO substrate. (c) The top view of the SEM photograph of the $CH_3NH_3PbI_3$ on $TiO_2$ nanorods/FTO. (d) The absorbance of the $TiO_2$ nanorods and the $CH_3NH_3PbI_3$ on $TiO_2$ nanorods/FTO.

Fig. 2(a) shows the *J*–*V* characteristics of the device. The cell delivered a short-circuit current density ($J_{sc}$) of 17.83 mA $cm^{-2}$, an open-circuit voltage ($V_{oc}$) of 0.76 V and a fill factor (FF) of 51.34%, leading to a very high PCE of 6.95%. We attribute this to the well-aligned band structure of the device (*i.e.*, the

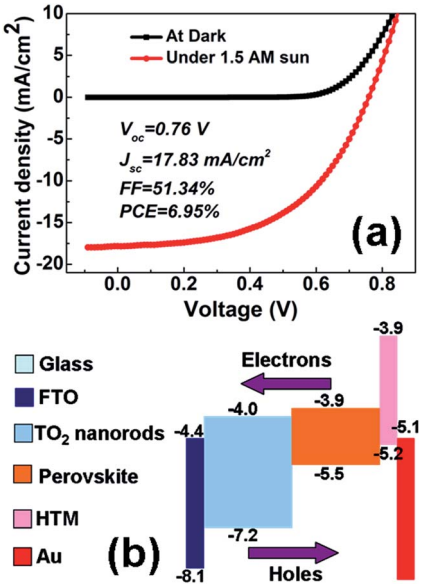


Fig. 2 (a) Current density *versus* voltage (*J*–*V*) plots of the perovskite-based photovoltaic device. (b) Energy band diagram of the perovskite-based solar cell.

fluorine-doped tin oxide (FTO), $TiO_2$, $CH_3NH_3PbI_3$, HTM and Au electron-affinities and Fermi levels are closely co-ordinated) (see Fig. 2(b)). This allows rapid charge-carrier separation at the interface, preventing photo-excited electrons in $TiO_2$ from recombining with holes at the p–n junction.

To investigate the self-powered photo-response characteristic of the $TiO_2$ NRs/$CH_3NH_3PbI_3$ heterojunction device, more detailed characteristics of the devices are shown in Fig. 3(a)–(d). Fig. 3(a) shows the *I–V* curves of the devices measured at dark and under illumination of 365 nm UV light, respectively. It shows that our diodes have large photocurrent under UV light with the current of ~15 μA at zero bias. The photoresponse behavior of the $TiO_2$ NRs/$CH_3NH_3PbI_3$ heterojunction is characterized by measuring the current as a function of time at zero bias when the light was periodically turned on and off, as shown in Fig. 3(b). From the figure, we can see that for each cycle, the "on"- and "off"-state currents remain the same within the noise level, which indicates the reversibility and stability of our PD. We can see that upon 365 nm UV illumination with light intensity of 17.2 μW $cm^{-2}$, the current increases quickly from ~−5 to ~−422 nA at 0 V, which indicates good UV photoresponse characteristic. And upon 546 nm visible-light illumination with light intensity of 37.9 μW $cm^{-2}$, the current increases to ~−750 nA at 0 V. And the ratio of photocurrent to dark current is as high as 150 at 546 nm. The spectral responses of $V_{oc}$ and $I_{sc}$ shown in Fig. 3(c) and (d) give another important characteristic of the self-powered PD. Both $V_{oc}$ and $I_{sc}$ display spectral responses from 300 to 800 nm, indicating that the device can be used as UV-visible PD.

The responsivity ($R$) and detectivity ($D^*$) are the important parameters to characterize the quality of the optimized PD. Based on the following equations

$$R = \frac{I_{ph}}{SP_{opt}} \quad (1)$$

$$D^* = \frac{R}{(2qJ_d)^{1/2}} \quad (2)$$

here, $I_{ph}$ is the photo-current, $S$ is the illuminated area, $P_{opt}$ is the light density, $J_d$ is the dark current and the shot noise from the dark current is the major contribution to the noise. The spectral responsivity and detectivity curves obtained under the biases of 0 V are presented in Fig. 4(a) and (b), respectively. From the curve of responsivity, our perovskite photodetector shows UV-visible response. The UV responses should be attributed to the $TiO_2$ due to its wide band gap, and the responses in visible region should be caused by the perovskite. Also we can see the responsivity shows two peaks located at 364 and 494 nm, respectively, which is the value of ~0.26 and 0.85 A $W^{-1}$ at 364 and 494 nm, respectively. Moreover, from 800 to 494 nm, the value of responsivity curve shows a continued increasing trend and reaches to the biggest at 494 nm, which is consistent with the report by Gao, *et al.*:[12] perovskite materials show strong light-capturing ability over the spectral region of 300–800 nm and in particular around 500 nm they can absorb more than 90% of incident light. Due to the low dark current of the device at zero bias, the perovskite photodetector shows good detection performance, which is shown in Fig. 4(b). We can see the peak detectivity of the perovskite photodetector is above 7.8 × $10^{10}$ cm $Hz^{1/2}$ $W^{-1}$ at 494 nm. The value of detectivity is slightly slow compared with the report,[8] we think the main reason is that the dark current of the device is a lot big and our following work will focus on the method of decreasing the dark current, such as an insertion layer applied in perovskite photodetector. From above, we conclude that the $TiO_2$ nanorods/$CH_3NH_3PbI_3$ heterojunction can work as a self-powered, ultraviolet-visible PD.

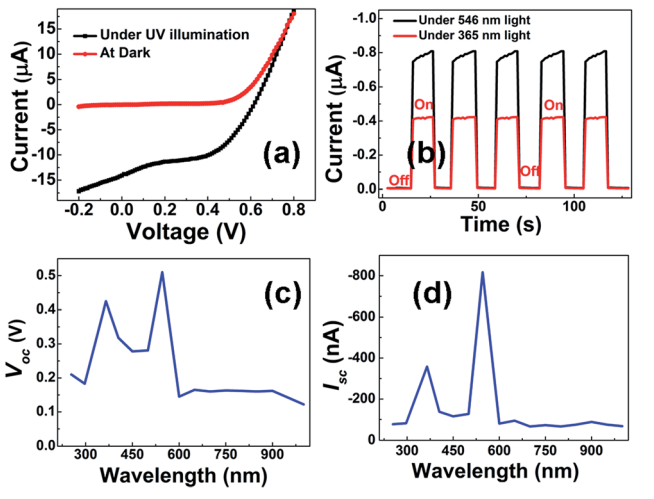


Fig. 3 (a) *I–V* characteristics of the perovskite-based PD under dark and 365 nm UV illumination. (b) The dependence of photocurrent on operating time for the PDs at zero bias. (c) The dependence of $V_{oc}$ on operating wavelength for the perovskite-based PDs. (d) The dependence of $I_{sc}$ on operating wavelength for the perovskite-based PDs.

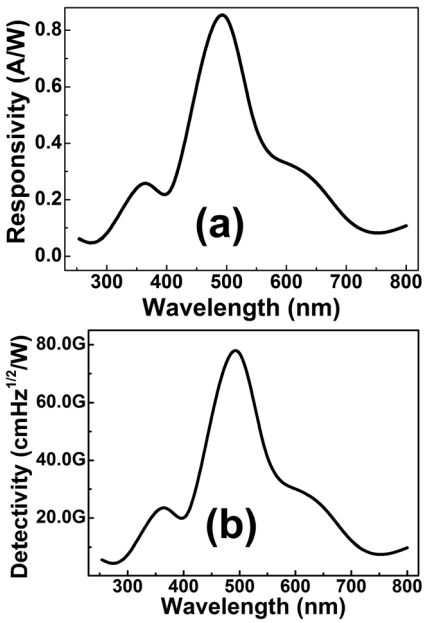


Fig. 4 (a) The spectral responsivity curve obtained under zero bias; (b) the spectral detectivity curve under zero bias.

The $TiO_2$ nanorods/$CH_3NH_3PbI_3$ heterojunction photodetector shows good self-powered, ultraviolet-visible photoresponse characteristics, the reason can be understood based on the energy level diagram (shown in Fig. 2(b)). It is clear that higher energy gaps and favorable energy alignment of $TiO_2$ and $CH_3NH_3PbI_3$ made them suitable candidates for photoresponse application. Under irradiation, the electron–hole pairs are generated when photon energy exceeds the energy band gap ($h\upsilon > E_g$). Photogenerated electrons flow from $TiO_2$ to the cathode. Although the perovskites have double carrier transport ability, the photogenerated electrons can not move from $CH_3NH_3PbI_3$ to the anode due to the block of the HTM, and the holes move from $CH_3NH_3PbI_3$ to the anode. These processes will contribute to a photocurrent at zero bias. With the increase of the absorption, more photons will be captured and generated more electron–hole pairs, leading to bigger current and better photoresponse characteristics. Due to the strong light-capturing ability of $CH_3NH_3PbI_3$ film in particular around 500 nm, the device shows the biggest value of responsivity near this wavelength. Although the absorption will increase with the decrease of the wavelength, responsivity will not increase, and the reason is that the shorter wavelengths are beyond its wavelength of the best photoelectric transformation efficiency due to the band-to-band transition of different electrons excited by different energy photons.[13]

## IV. Conclusion

In conclusion, a self-powered, ultraviolet-visible perovskite photodetector based on $TiO_2$ nanorods/$CH_3NH_3PbI_3$ heterojunction was fabricated. The device showed good photovoltaic properties with a short-circuit current density of 17.83 mA $cm^{-2}$, an open-circuit voltage of 0.76 V, a fill factor of 51.34% and a very high PCE of 6.95%. Also it displayed good ultraviolet-visible photo-response characteristic at zero bias, respectively.

## Acknowledgements

This work is supported in part by the National Nature Science Foundation of China (No. 51372075), Research Fund for the Doctoral Program of Higher Education of China (RFDP, No. 20124208110006), Natural Science Foundation of Hubei Province (No. 2014CFB538).

## References

1 D. B. Mitzi, *Prog. Inorg. Chem.*, 2007, **48**, 1–121.
2 H. Zhou, Q. Chen, G. Li, S. Luo, T. Song, H. Duan, Z. Hong, J. You, Y. Liu and Y. Yang, Interface engineering of highly efficient perovskite solar cells, *Science*, 2014, **345**(6196), 542–546.
3 M. Liu, M. B. Johnston and H. J. Snaith, Efficient planar heterojunction perovskite solar cells by vapour deposition, *Nature*, 2013, **501**(7467), 395–398.
4 N. J. Jeon, J. H. Noh, W. S. Yang, Y. C. Kim, S. Ryu, J. Seo and S. I. Seok, Compositional engineering of perovskite materials for high-performance solar cells, *Nature*, 2015, **517**, 476–480.
5 L. Etgar, P. Gao, Z. Xue, Q. Peng, A. K. Chandiran, B. Liu, M. K. Nazeeruddin and M. Grätzel, Mesoscopic $CH_3NH_3PbI_3/TiO_2$ Heterojunction Solar Cells, *J. Am. Chem. Soc.*, 2012, **134**(42), 17396–17399.
6 D. Bi, L. Yang, G. Boschloo, A. Hagfeldt and E. M. Johansson, Effect of Different Hole Transport Materials on Recombination in $CH_3NH_3PbI_3$ Perovskite-Sensitized Mesoscopic Solar Cells, *J. Phys. Chem. Lett.*, 2013, **4**(9), 1532–1536.
7 G. E. Eperon, V. M. Burlakov, P. Docampo, A. Goriely and H. J. Snaith, Morphological Control for High Performance, Solution-Processed Planar Heterojunction Perovskite Solar Cells, *Adv. Funct. Mater.*, 2014, **24**(1), 151–157.
8 L. Dou, Y. (Micheal) Yang, J. You, Z. Hong, W.-H. Chang, G. Li and Y. Yang, Solution-processed hybrid perovskite photodetectors with high detectivity, *Nat. Commun.*, 2014, **5**, 5404.
9 X. Hu, X. Zhang, L. Liang, J. Bao, S. Li, W. Yang and Y. Xie, High-Performance Flexible Broadband Photodetector Based on Organolead Halide Perovskite, *Adv. Funct. Mater.*, 2014, **24**(46), 7373–7380.
10 H. R. Xia, J. Li, W. T. Sun and L. M. Peng, Organohalide lead perovskite based photodetectors with much enhanced performance, *Chem. Commun.*, 2014, **50**(89), 13695–13697.
11 X. Li, C. Gao, H. Duan, B. Lu, X. Pan and E. Xie, Nanocrystalline $TiO_2$ film based photoelectrochemical cell as self-powered UV-photodetector, *Nano Energy*, 2012, **1**, 640.
12 X. Gao, J. Li, J. Baker, Y. Hou, D. Guan, J. Chen and C. Yuan, *Chem. Commun.*, 2014, **50**, 6368–6371.
13 H. Zhou, J. Mei, P. Gui, P. Tao, Z. Song, H. Wang and G.-J. Fang, The investigation of Al-doped ZnO as an electron transporting layer for visible-blind ultraviolet photodetector based on n-ZnO nanorods/p-Si heterojunction, *Mater. Sci. Semicond. Process.*, 2015, **38**, 67–71.

 